Journal of Physics: Conference Series **607** (2015) 012014 doi:10.1088/1742-6596/607/1/012014

Overview of Higgs boson results from ATLAS experiment at the LHC

I.I. Tsukerman on behalf of the ATLAS Collaboration
ITEP, Moscow, 117218, Russia
E-mail: ilya.tsukerman@cern.ch

Abstract. One year ago, a new particle with the mass of 125 GeV and properties expected for the Standard Model Higgs boson was discovered by ATLAS and CMS experiments at the Large Hadron Collider at CERN in proton-proton collisions at center-of-mass energies $\sqrt{s}$ =7 TeV and 8 TeV. Since that time more data at 8 TeV were accumulated and analyzed and a progress was reached in the measurement of the particle properties. In this note an overview of Higgs boson results obtained recently at ATLAS experiment is given. Complete dataset which corresponds to 4.7 fb^{-1} (20.5 fb^{-1}) of the data obtained at $\sqrt{s}$ =7 TeV (8 TeV) collisions, respectively, is used. The following four signal decay channels are considered: $H \to \gamma\gamma$, $H \to ZZ^\star \to 4\ell$, $H \to WW^\star \to \ell\ell\nu\nu$ and $H \to b\bar{b}$. These channels together with $H \to \tau\tau$ channel are combined to extract Higgs boson mass, strength, coupling constants, spin and parity. All experimental results are compatible with the Standard Model predictions.

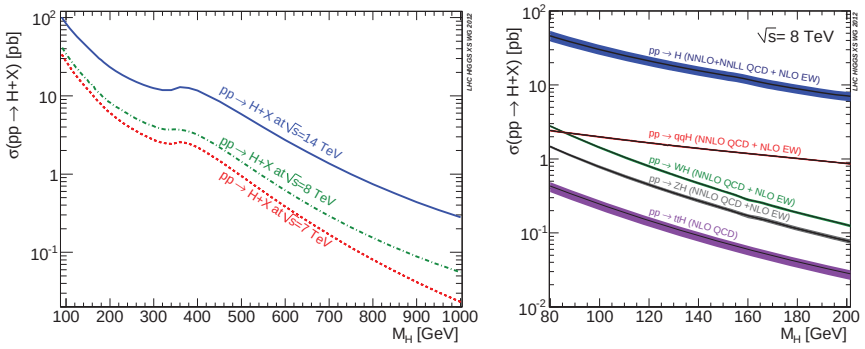
1. Introduction

The search for the Standard Model (SM) Higgs boson (H) at the Large Hadron Collider (LHC) is known to be complicated task as expected signal production cross section is σ_H =O(10) pb while background rates are much higher. Fig.1(a) shows how predicted σ_H depends on its mass at different center-of-mass pp energies, $\sqrt{s}$ =7 TeV, 8 TeV and 14 TeV [1] which correspond to the LHC conditions in 2011, 2012 and 2015 year, respectively. It is about 15 pb at m_H =125 GeV at $\sqrt{s}$ =7 TeV being 1.3 times higher at $\sqrt{s}$ =8 TeV. At larger m_H the cross section increases with $\sqrt{s}$ stronger. There are four main mechanisms of H production at LHC energies: gluon-gluon fusion (ggF) via heavy-quark triangular loop, vector-boson fusion (VBF) where Higgs boson is accompanied by two energetic jets going at small polar angles, associated production with one vector boson (VH, i.e. together with W or Z) and top-antitop fusion. The expected σ_H in these mechanisms is shown in Fig.1(b) as function of m_H at $\sqrt{s}$=8 TeV together with theoretical uncertainties [1]. The σ_H was calculated in NNLO approximation (except $t\bar{t}H$ process for which NLO approach is used). It is seen that the ggF mechanism dominates while rates via VBF (VH, $t\bar{t}H$) mechanisms are ten (a few dozens, hundred) times smaller, respectively.

Expected branching ratios (BR) of the experimentally favourable decay modes multiplied by σ_H at 8 TeV are shown in Fig.2(a). They are as large as 1.5 pb at m_H =125 GeV for $H \to \tau\tau$ and $H \to WW^\star \to \ell\nu q\bar{q}$ channels. However, signal-to-background (S/B) ratios for these channels are small and mass reconstruction is problematic. $H \to WW^\star \to \ell\nu\ell\nu$ channel has lower cross section, 0.25 pb, but one can reach sizeable S/B ratio doing kinematical selections. Again, mass reconstruction looks non-trivial. $H \to \gamma\gamma$ channel has very good and simple signature. Hovewer, $\sigma_H \times BR(H \to \gamma\gamma)$ is less than 0.05 pb, and background conditions

Content from this work may be used under the terms of the Creative Commons Attribution 3.0 licence. Any further distribution of this work must maintain attribution to the author(s) and the title of the work, journal citation and DOI.
Published under licence by IOP Publishing Ltd

are very hard. The most clean decay mode, where both signature and S/B ratio are perfect is $H \to ZZ^\star \to 4\ell$. But $\sigma_H \times BR(H \to 4\ell)$ is only a few pb due to small leptonic branching ratio of the Z boson. Despite these difficulties, both ATLAS [2] and CMS [3] Collaborations



(a) (b)

Figure 1. (a) Predicted total σ_H at $\sqrt{s}$ =7, 8 and 14 TeV as function of m_H. (b) Predicted total σ_H at $\sqrt{s}$ =8 TeV together with separate contributions from different production mechanisms as function of m_H.

at the LHC were able to discover one year ago a new particle with properties of SM-like Higgs boson combining $H \to \gamma\gamma$, $H \to ZZ^\star \to 4\ell$ and $H \to WW^\star \to \ell\ell\nu\nu$ decay channels. Their studies were based on complete data taken at 7 TeV ($\approx$5 fb^{-1}) and on one third of 8-TeV dataset ($\approx$6 fb^{-1}). Currently, preliminary analyses of full 8 TeV data are advanced and corresponding results are started to appear. Summary presented in this note is based on complete 7-TeV and 8-TeV ATLAS datasets. The note is organized as follows. The ATLAS detector is briefly described in Section 2. In Section 3, the most interesting decay modes of the SM Higgs boson, namely $H \to \gamma\gamma$, $H \to ZZ^\star \to 4\ell$, $H \to WW^\star \to \ell\ell\nu\nu$ and $H \to b\bar{b}$ are considered; results of statistical combination of these channels together with $H \to \tau\tau$[1] are presented in Section 4. This combination includes particle mass, signal strength, coupling constants, spin and parity.

2. The ATLAS detector and its modeling

The ATLAS detector [4] is a multipurpose particle physics apparatus with forward-backward symmetric cylindrical geometry. The inner tracking detector is surrounded by a thin superconducting solenoid which provides a 2 T magnetic field, and by electromagnetic (EM) and hadronic calorimetry. The calorimeters are divided into a central barrel and end-cap regions on either end of the detector covering the range $|\eta| \leq 4.9$.[2] In the central region $|\eta| \leq 1.8$, the EM calorimeter is preceded by a presampler detector to correct for upstream energy losses. The muon spectrometer surrounds the calorimeters and consists of three air-core superconducting magnets providing a toroidal field, a system of precision tracking chambers, and fast detectors for triggering. The combination of all these systems provides charged particle measurements together with efficient and precise lepton and photon measurements in the range $|\eta| \leq 2.5$.

[1] For this particular channel, one-year-old results are used in the combination.

[2] ATLAS uses a right-handed coordinate system with the origin at the nominal interaction point (IP) in the centre of the detector, and the z-axis along the beam line. The x-axis points from the IP to the centre of the LHC ring, and the y-axis points upwards. Cylindrical coordinates (r, θ) are used in the transverse plane, θ being the azimuthal angle around the beam line. Observables labelled "transverse" are projected into the $x - y$ plane. The pseudorapidity is defined in terms of the polar angle θ, as $\eta = \ln\tan(\theta/2)$.

Jets and missing transverse energy, E_T^{miss}, are reconstructed using energy deposits over the full coverage of the calorimeters. To develop analysis procedures, to calculate signal acceptance and to evaluate contribution for some background processes, Monte-Carlo (MC) modeling is used. All simulated signal and background datasets are passed through GEANT4 [5] full simulation chain of ATLAS set-up and algorithms used also in real data recontruction. Multiple interactions in the same bunch crossing[3] including detector effects are also modeled. In many cases backgrounds are directly **measured** experimentally in the so-called control regions, kinematically orthogonal to signal regions. Corresponding normalization factors are determined from simulation.

3. $H \to \gamma\gamma$, $H \to ZZ^\star \to 4\ell$, $H \to WW^\star \to \ell\ell\nu\nu$ and $H \to b\bar{b}$ decay channels

3.1. $H \to \gamma\gamma$ *[6], [7], [8]*

The expected cross section of $H \to \gamma\gamma$ production and decay is 30–50 fb in the region m_H =110–150 GeV. At higher Higgs boson masses it falls rapidly mainly due to strong decrease of the BR($H \to \gamma\gamma$). The signature is two high-p_T isolated photons with invariant mass $m_{\gamma\gamma} = m_H$. Simulations show that the ATLAS EM calorimeter allows to reach invariant-mass resolution $FWHM \approx 4$ GeV in the region of interest. Irreducible background consists of continuum production of photon pairs via $q\bar{q} + gg \to \gamma\gamma$ mechanisms. These processes have about hundred times larger rates than expected for the signal. Reducible backgrounds include mostly γjet- and $jetjet$-production when one or two jets are misidentified as photons in the detector. These processes have many orders of magnitude higher cross sections than the continuum diphoton production. Thanks to the EM calorimeter with a preshower, one can reach required jet rejection at the level of 10^4. Some 13K events survive all the selections while expected signal in the mass window around 125 GeV is $\approx$ 400. To increase discovery potential, the events are further subdivided into fourteen independent categories having different expected $m_{\gamma\gamma}$ resolution and S/B ratio. The $m_{\gamma\gamma}$-distribution after corresponding reweighting is given in Fig.2(b) together with the spectrum after background subtraction. Excess of events is seen around 126 GeV. The probability that background fluctuation causes at least observed excess of events, called p_0, is shown in Fig.3(a) as function of m_H. A clear signal at around 126.5 GeV with 7.4σ local significance is seen. The measured mass of the new particle is 126.8$\pm$0.2 (stat)$\pm$0.7 (syst) GeV, where systematic error is mainly due to photon energy scale uncertainty. Taking into account known Landau-Yang theorem, this particle cannot have spin equal to one. The measured signal strengths in units of the SM for VH, VBF and ggF+$t\bar{t}H$ couplings separately, are the following: $\mu_{ggF+t\bar{t}H} \times B/B_{SM}$ =$1.6^{+0.3}_{-0.3}(\text{stat})^{+0.3}_{-0.2}$(syst); $\mu_{VBF} \times B/B_{SM}$ =$1.7^{+0.8}_{-0.8}(\text{stat})^{+0.5}_{-0.4}$(syst) and $\mu_{VH} \times B/B_{SM}$ =$1.8^{+1.5}_{-1.3}(\text{stat})^{+0.3}_{-0.3}$(syst). Combining them one obtains the value μ =1.65$\pm$0.24 $(\text{stat})^{+0.25}_{-0.18}$ (syst) which is 2.3σ away from the SM prediction of one.

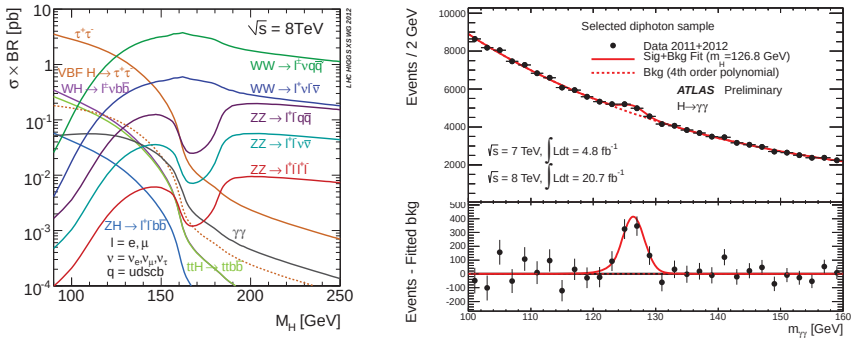
Using kinematical distributions in the so-called Collins-Soper frame one can exclude a possibility of spin-2 of newly observed particle [7]. The obtained log-likelihood ratio of spin-0 and spin-2 hypotheses is given in Fig.3(b) as function of $f_{q\bar{q}} = \sigma_H^{q\bar{q}}/\sigma_H^{total}$. One can see that the spin-2 hypothesis[4] is excluded at 99% CL assuming that all signal events are produced through gg-fusion. This number is reduced to 95% if 25% admixture of $q\bar{q}$ events is supposed.

In Ref.[8] distributions on kinematic variables in di-photon signal candidates are analyzed and compared with theoretical models. No big deviation from the SM prediction is observed.

3.2. $H \to ZZ^\star \to 4\ell$ *[9]*

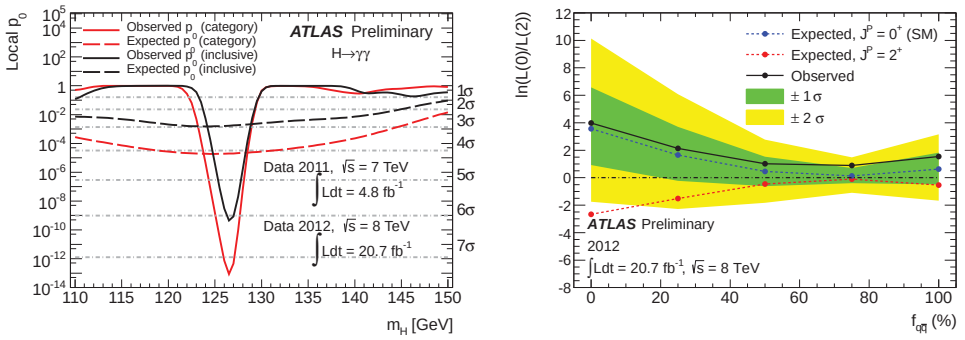
$H \to ZZ^\star \to 4\ell$ decay mode is promising when searching for the SM Higgs boson in a wide mass range from 110 GeV to 600 GeV. The $\sigma_H \times BR(H \to 4\ell)$ is 3 fb at m_H =125 GeV for $\sqrt{s}$=8 TeV. Signal signature is two pairs of isolated, high p_T opposite-sign leptons (electrons or muons);

[3] In average, ten (twenty) interactions occurred each 50 ns in the same bunch crossing at $\sqrt{s}$=7 TeV (8 TeV).
[4] Graviton-like model is used to simulate the spin-2 case.



(a) (b)

Figure 2. (a) $\sigma_H \times BR(H \to X)$ at $\sqrt{s}$ =8 TeV for the most promising decay channels X as function of m_H. (b) $m_{\gamma\gamma}$-distribution for the combined 7-TeV and 8-TeV data samples in $H \to \gamma\gamma$ searches. The bottom inset displays the residuals of the data with respect to the fitted background component.

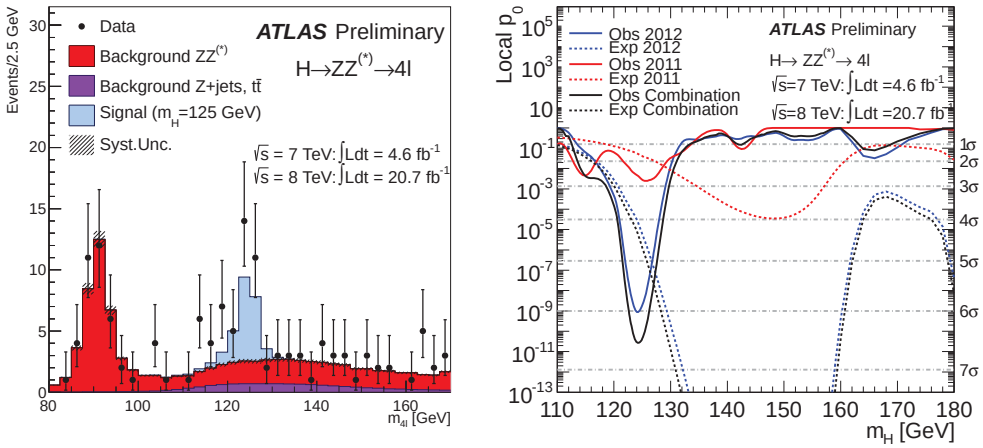


(a) (b)

Figure 3. Results of the $H \to \gamma\gamma$ study. (a) The observed local p_0 value as function of m_H for the combination of 7-TeV and 8-TeV data for the inclusive case (black) and for the analysis using categories (red). (b) Median expected values of the test statistics $ln(L(0)/L(2))$ for the spin-0 (dashed blue/upper line and corresponding 68% and 95% CL bands) and spin-2 (dashed red/lower line) hypotheses, as well as the observed values (solid line) as function of the $f_{q\bar{q}}$.

at least one pair should have $m_{\ell\ell} = m_Z$. Irreducible backgrounds come from $q\bar{q} + gg \to ZZ^\star$ processes which have comparable cross sections with the expected signal at 125 GeV. Smaller reducible backgrounds are due to $t\bar{t}$ and Drell-Yan production. ATLAS detector has excellent four-lepton invariant-mass resolution, namely 1.6 GeV (1.9 GeV, 2.4 GeV) for the 4μ (2μ2e, 4e) cases, respectively. The measured invariant-mass distribution, $m_{4\ell}$, after combination of all the lepton cases is shown in Fig.4(a). Clear maximum above background is seen in the region around 125 GeV; 32 events are observed in the mass window 125±5 GeV with the estimated background 11.1±1.0 events. The data/MC ratio is compatible with unity in the sidebands. The peak at $m_{4\ell} = m_Z$ is due to rare Z boson decay to four leptons. The p_0 probability is shown in Fig.4(b) as function of m_H in the region 110–180 GeV. The local significance reaches 6.6σ at 124 GeV and no other big fluctuations are observed in the mentioned mass range. The reconstructed mass of the new particle is 124.3±0.6 (stat)±0.4 (syst) GeV. The measured signal

strength, μ =1.7±0.4, is compatible with the SM prediction of one at 2σ level. In addition, SM-like Higgs boson is excluded at 95% CL with the mass below 650 GeV (350 GeV) in the ggF (VBF) mechanisms alone [9]. Despite signal statistics is small, the excellent S/B ratio allows to study such properties of the signal as spin and parity using angular distributions of the newly observed particle's decay products. Six spin-parity hypotheses are tested: 0^+ (as predicted by the SM), 0^-, 1^+, 1^-, 2^+ and 2^-. The events passed all kinematical selections which have 115 GeV$\leq m_{4\ell} \leq$130 GeV are used in this study. Two analyses were performed. The first one is based on Boosted Decision Tree (BDT) and the second one is based on matrix element likelihood ratio (J^P-MELA). Log-likelihood ratios are presented in Table 1 for all the spin-parity cases as



(a) (b)

Figure 4. Results of the $H \to ZZ^\star \to 4\ell$ study. (a) $m_{4\ell}$ distributions for the selected candidates compared to the background expectation in the mass range 80-170 GeV. The signal expectation for the m_H =125 GeV hypothesis is also shown. (b) The observed local p_0-value for the combination of the 2011 and 2012 data sets (solid black line); the $\sqrt(s)$ =7 TeV and 8 TeV data results are shown in solid lines (blue and red, respectively).

well as for the BDT-based and MELA-based analyses separately. One can see that the 0^- and 1^+ hypotheses are strongly disfavoured with respect to the 0^+ hypothesis. However, exclusion of the 2^+ case is less effective. The 0^+ and 2^+ hypotheses are also compared assuming different $f_{q\bar{q}}$ fraction [9].

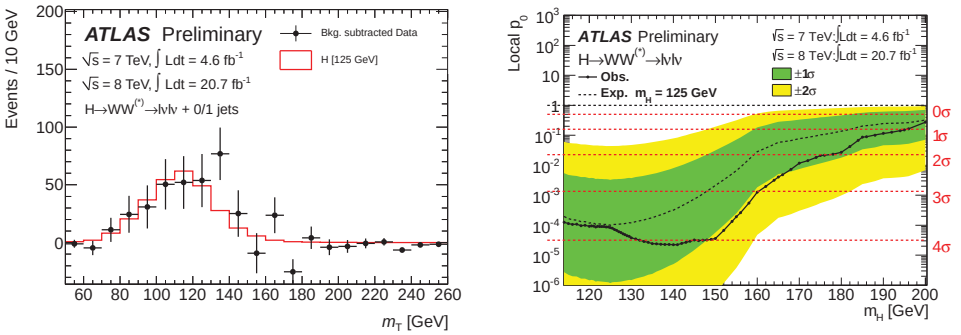
3.3. $H \to WW^\star \to \ell\ell\nu\nu$ decay channel [10], [11], [12], [13]

$H \to WW^\star \to \ell\ell\nu\nu$ decay channel has expected cross section of about 250 fb at 8 TeV for m_H =125 GeV. The search mass range is 110–200 GeV. The signature is two high-p_T isolated opposite-sign leptons and large E_T^{miss} due to neutrinos so one cannot reconstruct Higgs boson mass. Instead, its transverse mass reconstruction is possible. It is calculated as $m_T = \sqrt{(E_T^{\ell\ell} + E_T^{miss})^2 - |\mathbf{P_T^{\ell\ell}} + \mathbf{E_T^{miss}}|^2}$, where $E_T^{\ell\ell} = \sqrt{|P_T^{\ell\ell}|^2 + m_{\ell\ell}^2}$, $P_T^{\ell\ell}$ ($m_{\ell\ell}$) is transverse momentum (invariant-mass) of the di-lepton system, respectively. So knowledge of background normalization and shapes is of importance. Backgrounds come from $q\bar{q} + gg \to WW$ continuum production as well as from $t\bar{t}$, Wt and Z+jets processes with di-lepton final state. W+jets with a jet misidentified as a lepton has also sizeable rate. Separate control regions for each of these backgrounds are defined to measure them. Event sample is subdivided in accordance with number of jets (0, 1 or ≥2) and di-lepton flavour (ee, $\mu\mu$ or eμ). For the 0 and 1 jet cases the

Table 1. For an assumed 0^+ hypothesis, the values for the expected and observed p_0-values of the different tested spin and parity hypotheses for the BDT and J^P-MELA analyses of the $H \to 4\ell$ channel. The results are given combining the 8 TeV and 7 TeV data sets. Also given is the observed p_0-value where 0^+ is the test hypothesis and the other spins states are the assumed hypothesis ("observed"). These two observed p_0-values are combined to provide the CL_s confidence level for each test hypothesis. The production mode is assumed to be 100% ggF.

	BDT analysis				MELA analysis			
	tested J^P for assumed 0^+		tested 0^+ for assumed J^P	CL_s	tested J^P for assumed 0^+		tested 0^+ for assumed J^P	CL_s
	expected	observed	observed		expected	observed	observed	
0^-p_0	0.0037	0.015	0.31	0.022	0.0011	0.0022	0.40	0.004
1^+p_0	0.0016	0.001	0.55	0.002	0.0031	0.0028	0.51	0.006
1^-p_0	0.0038	0.051	0.15	0.060	0.0010	0.027	0.11	0.031
2^+p_0	0.092	0.079	0.53	0.168	0.064	0.11	0.38	0.182
2^-p_0	0.0053	0.25	0.034	0.258	0.0032	0.11	0.08	0.116

ggF mechanism is expected to dominate while for the multi-jet case signal events are mostly due to the VBF mechanism. The m_T-distribution after background subtraction is shown in Fig.5(a). Clear excess of events is seen in the region 80–140 GeV. The local p_0 as function of m_H is shown in Fig.5(b). It corresponds to 3.8σ signal significance at 126 GeV. The fitted signal strength is equal to 1.0±0.3, i.e. compatible with the SM prediction. 95% CL of signal exclusion is reached (expected) in the region above 134 (118) GeV.



(a) (b)

Figure 5. Results of the $H \to WW^\star \to \ell\ell\nu\nu$ study. (a) Background-subtracted m_T distribution. The signal is overlaid. The error bars represent the statistical uncertainties of the data and the subtracted background; it does not include the systematic uncertainties of the latter. (b) Results for the p_0 as function of m_H. The smaller green bands represent 1σ uncertainties on the expected values, and the larger yellow bands represent 2σ uncertainties.

Spin-parity properties are also studied with the $H \to WW^\star \to \ell\ell\nu\nu$ decay channel [11]. Two hypotheses were considered: 0^+ and 2^+. To discriminate between them, multivariate analysis based on four variables ($m_{\ell\ell}$, $\Delta\phi\ell\ell$, $P_T^{\ell\ell}$ and m_T), was performed.[5] Depending on the $f_{q\bar{q}}$ fraction,

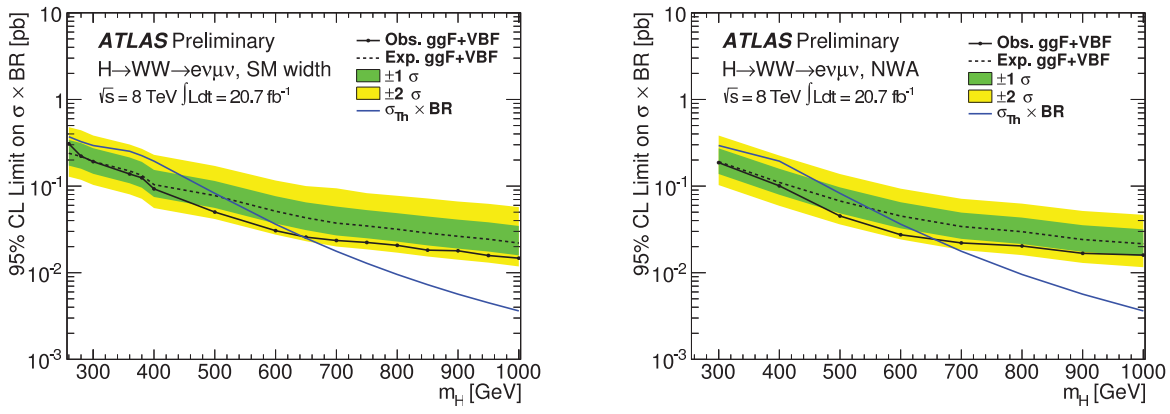
[5] $\Delta\phi_{\ell\ell}$ is azimuthal angle gap between leptons.

exclusion of the 2^+ hypothesis at the CL between 95% and 99% is reached.

In addition, the search for $H \to WW \to \ell\ell\nu\nu$ in the high-mass region 260–1000 GeV is made [12]. The predicted $\sigma_H \times BR(H \to WW \to \ell\ell\nu\nu)$ at 8 TeV decreases from 300 fb at m_H =260 GeV to 4 fb at m_H =1000 GeV. Selection criteria were specially optimized to high-mass searches and a cut-based analysis is performed. Only $H \to WW \to e\nu\mu\nu$ channel is considered. Two extreme Higgs boson lineshapes are taken: the SM-like, i.e. from the Complex Pole Scheme (CPS), and zero width, i.e. from the Narrow Width Approximation (NWA). Corresponding exclusion plots are shown in Fig.6(a) and in Fig.6(b), respectively. SM-like Higgs boson with $m_H \leq 642$ GeV is excluded at 95% CL; a bit higher value is obtained for the NWA case.

At last, associated VH-production with subsequent $H \to WW \to \ell\ell\nu\nu$ decay is investigated in the range 110 GeV$\leq m_H \leq$200 GeV [13]. To have better S/B ratio, Z (W) bosons are tagged via their $\ell\ell$ ($\ell\nu$) decays, respectively. Expected signal cross section is about 1.8 fb at m_H =125 GeV. The signature is three or four isolated, high-p_T leptons and large E_T^{miss}. Backgrounds include WWW-, and WZ/γ^*- and ZZ-production as well as other di-lepton final states with additional fake lepton. The study has shown that $\sigma_H \leq 7.2\sigma_{SM}$ is excluded at 95% CL for m_H =125 GeV. With the inclusion of VH-production, the combined $H \to WW \to \ell\ell\nu\nu$ signal significance increases from 3.8σ to 4.0σ.

3.4. VH, $H \to b\bar{b}$ decay channel [14]



(a) (b)

Figure 6. 95% CL upper limits on $\sigma_H \times BR(H \to WW \to e\nu\mu\nu)$ at 8 TeV for a Higgs boson with (a) a SM-like lineshape and (b) a narrow lineshape (NWA). The green and yellow bands show the 1σ and 2σ uncertainties on the expected limit. The expected cross section times branching ratio for the production of a SM Higgs boson is shown as a blue line.

Among all channels, $H \to b\bar{b}$ is predicted to have the largest rate in the mass range 110–150 GeV. However, background is known to be huge. For this reason, here associated VH-production is of interest. The signature includes two energetic jets originating from b-quarks having invariant-mass $m_{b\bar{b}}$ close to m_H as well as one or two high-p_T leptons or large E_T^{miss} depending on the decay mode of the associated vector boson ($W \to \ell\nu$, $Z \to \ell\ell$, $Z \to \nu\nu$, respectively). Backgrounds consist of W/Z+ jets, dibosons, top and multijet production with fake leptons. Reconstructed $m_{b\bar{b}}$ is shown in Fig.7(a) after subtraction of all backgrounds except dibosons. No significant deviation of the data from simulations is seen. $1.4\sigma_{SM}$ cross section

is excluded at 95% CL for m_H =125 GeV, see Fig.7(b). The measured signal strength is μ =0.2±0.5(stat)±0.4(sys).

4. Statistical combination of $H \to \gamma\gamma$, $H \to ZZ^\star \to 4\ell$, $H \to WW^\star \to \ell\ell\nu\nu$, $H \to b\bar{b}$ and $H \to \tau\tau$ decay channels

4.1. Signal strength, reconstructed mass and measured couplings [15], [16], [17]

The local probability p_0 for a background-only experiment to be more signal-like than the observation as function of m_H for the combination of all channels is shown in Fig.8(a). The observed local significance is 10σ and the expected significance at m_H =125 GeV is 7.5σ [16]. The measured signal mass based on $H \to \gamma\gamma$ and $H \to ZZ^\star \to 4\ell$ channels is m_H^{obs} =125.5±0.2±0.6 GeV with 2.5σ tension between the values predicted from these separate channels [15][6]. The combined signal strength in units of the σ_{SM}, μ, is measured to be 1.33±0.14(stat)±0.15(sys) from three channels $H \to \gamma\gamma$, $H \to ZZ^\star \to 4\ell$ and $H \to WW^\star \to \ell\ell\nu\nu$. If the preliminary $H \to \tau\tau$ [18] and $H \to b\bar{b}$ [19] results, for which only part of the 8 TeV data is used (13 fb^{-1}), were included, the combined signal strength would be μ =1.23±0.18.

Since several Higgs boson production modes are available at the LHC, one can measure separately two signal strength parameters in units of corresponding SM-predicted cross sections, $\mu_{ggF+ttH} = \mu_{ggF} = \mu_{ttH}$ from gluon-mediated processes and $\mu_{VBF+VH} = \mu_{VBF} = \mu_{VH}$ from vector-boson-mediated processes. A ratio $\mu_{VBF+VH}/\mu_{ggF+ttH} = 1.4^{+0.7}_{-0.5}$ is obtained from the combination of three channels, $H \to \gamma\gamma$, $H \to WW^\star \to \ell\ell\nu\nu$ and $H \to ZZ^\star \to 4\ell$. This result provides evidence at the 3.3σ level that a fraction of H production occurs through the VBF.

Measurements of couplings are implemented using a leading-order tree-level motivated framework with some assumptions [17]. The coupling scale factors κ_j are defined in such a way that the cross sections σ_j and the partial decay widths Γ_j associated with the SM particle j scale with κ^2 compared to the SM prediction. Assuming one coupling scale factor for fermions, κ_F, and one for bosons, κ_V, the 68% CL intervals profiling over the other parameter, are $\kappa_F \in$[0.76,1.18] and $\kappa_V \in$[1.05,1.22]. If we relax the assumption that there are no contributions from new particles to the Higgs boson width, only the ratio $\lambda_{FV} = \kappa_F/\kappa_V$ can be measured which still provides useful information on the relationship between Yukawa and gauge couplings. Fits to the data give the following 68% CL intervals for λ_{FV} and $\kappa_{VV} = \kappa_V\kappa_V/\kappa_H$: $\lambda_{FV} \in$[0.70,1.01] and $\kappa_{VV} \in$[1.13,1.45].

Many BSM physics scenarios predict the existence of new heavy particles, which can contribute to loop-induced processes such as ggF production and $H \to \gamma\gamma$ decay. Effective scale factors κ_g and κ_γ are introduced to parameterise the ggF and $H \to \gamma\gamma$ loops. The best-fit values when profiling over the other parameters are: κ_g =1.04±0.14 and κ_γ =1.20±0.15.

In summary, no significant deviation from the SM prediction is observed in any of the measurements performed.

4.2. Spin combination [20], [21]

The three H decay channels are combined to study spin properties of the observed new boson: $H \to \gamma\gamma$, $H \to ZZ^\star \to 4\ell$ and $H \to WW^\star \to e\nu\mu\nu$. Complete 8-TeV dataset is used for this study; for the $H \to ZZ^\star \to 4\ell$ channel all data obtained at 7 TeV are added. Five different spin-parity hypotheses were tested: 0^+, 0^-, 1^+, 1^-, and 2^+. Data strongly favour the 0^+ hypothesis. 1^+ and 2^+ hypotheses are excluded with CL≥99.9%, see Fig.8(b). Table 2 shows the expected and observed p_0 values for both the 0^+ and 2^+ hypotheses for the combination of mentioned channels. The results are shown as function of the $f_{q\bar{q}}$ production fraction.

[6] $\Delta m_H = m_H(\gamma\gamma) - m_H(4\ell)$ =2.3±0.7(stat)±0.6(sys) GeV.

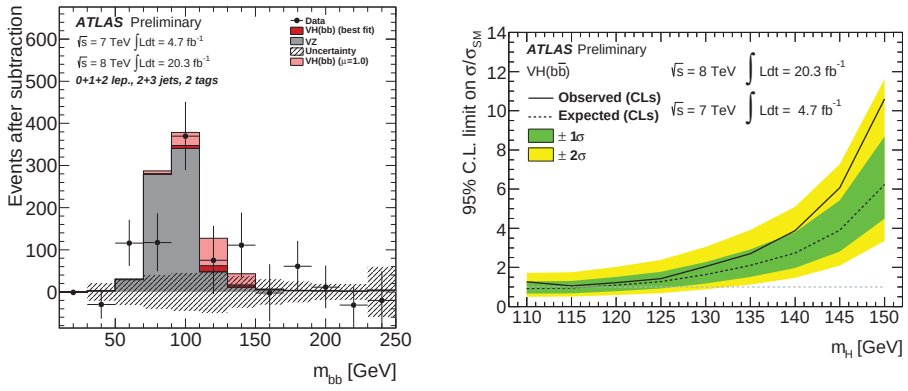
Table 2. Expected and observed p_0 values for the 0^+ and 2^+ hypotheses as function of the $f_{q\bar{q}}$ of the spin-2 production mechanism in the combined H study. The values are calculated for the combination of the three H decay channels. The CLs values are also presented.

$f_{q\bar{q}}$	2^+ assumed exp. $p_0(J^P=0^+)$	0^+ assumed exp. $p_0(J^P=2^+)$	obs. p_0 $(J^P=0^+)$	obs. p_0 $(J^P=2^+)$	CL_s $(J^P=2^+)$
100%	3.0×10^{-3}	8.8×10^{-5}	0.81	1.6×10^{-6}	0.8×10^{-5}
75%	9.5×10^{-3}	8.8×10^{-4}	0.81	3.2×10^{-5}	1.7×10^{-4}
50%	1.3×10^{-2}	2.7×10^{-3}	0.84	8.6×10^{-5}	5.3×10^{-4}
25%	6.4×10^{-3}	2.1×10^{-3}	0.80	0.9×10^{-4}	4.6×10^{-4}
0%	2.1×10^{-3}	5.5×10^{-4}	0.63	1.5×10^{-4}	4.2×10^{-4}

5. Conclusion

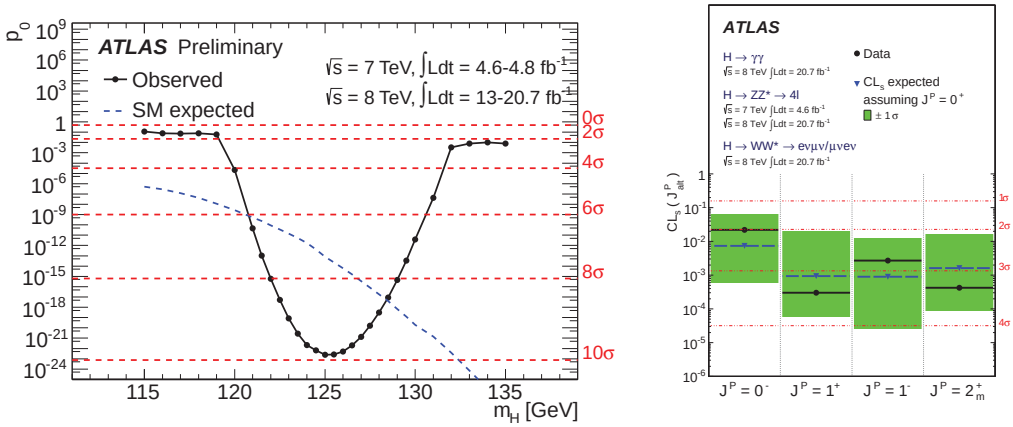
- Based on analysis of $H \to \gamma\gamma$, $H \to ZZ^\star \to 4\ell$, $H \to WW^\star \to \ell\ell\nu\nu$ decay channels in complete dataset taken at $\sqrt{s}$ =7 TeV and 8 TeV, the ATLAS experiment discovered neutral boson with a mass ≈125 GeV which has production cross section compatible with the SM Higgs boson; fermionic decay modes of this boson are not yet discovered;
- First measurements of the new boson couplings were performed and they are all in agreement with the SM predictions; coupling to bosons were measured with much better precision than couplings to fermions;
- Different spin/parity hypotheses of the new particle were tested and the one predicted by the SM, $J^P=0^+$ hypothesis, has strong preference;
- ATLAS is continuing to study properties of the discovered boson and plan to improve the measurements with new data expected starting from year 2015. An overview of the expected measurement precision in each channel for the signal strength μ and its coupling constants at 14-TeV LHC with respect to the SM H with m_H =125 GeV is given in Ref.[22].

[1] Dittmaier S et al, http://arxiv.org/abs/1101.1593
[2] ATLAS Collaboration, 2012 *Phys. Lett. B* **716** 1.
[3] CMS Collaboration, 2012 *Phys. Lett. B* **716** 30.
[4] ATLAS Collaboration, 2008 JINST **3** S08003.
[5] Allison J et al, 2006 *IEEE Trans. Nucl. Sci.* **53** 270; Agostinelli S et al, 2003 *NIM A* **506** 250.
[6] ATLAS Collaboration, 2013 ATLAS-CONF-2013-012, http://cds.cern.ch/record/1523698
[7] ATLAS Collaboration, 2013 ATLAS-CONF-2013-029, http://cds.cern.ch/record/1527124
[8] ATLAS Collaboration, 2012 ATLAS-CONF-2012-168, http://cds.cern.ch/record/1499625
[9] ATLAS Collaboration, 2013 ATLAS-CONF-2013-013, http://cds.cern.ch/record/1523699
[10] ATLAS Collaboration, 2013 ATLAS-CONF-2013-030, http://cds.cern.ch/record/1527126
[11] ATLAS Collaboration, 2013 ATLAS-CONF-2013-031, http://cds.cern.ch/record/1527127
[12] ATLAS Collaboration, 2013 ATLAS-CONF-2013-067, http://cds.cern.ch/record/1562879
[13] ATLAS Collaboration, 2013 ATLAS-CONF-2013-075, http://cds.cern.ch/record/1562933
[14] ATLAS Collaboration, 2013 ATLAS-CONF-2013-079, http://cds.cern.ch/record/1563235
[15] ATLAS Collaboration, 2013 ATLAS-CONF-2013-014, http://cds.cern.ch/record/1523727
[16] ATLAS Collaboration, 2013 ATLAS-CONF-2013-034, http://cds.cern.ch/record/1528170
[17] ATLAS Collaboration, 2013 *Phys. Lett. B* **726** 88. http://arxiv.org/pdf/1307.1427
[18] ATLAS Collaboration, 2012 ATLAS-CONF-2012-160, http://cds.cern.ch/record/1493624
[19] ATLAS Collaboration, 2012 ATLAS-CONF-2012-161, http://cds.cern.ch/record/1493625
[20] ATLAS Collaboration, 2013 ATLAS-CONF-2013-040, http://cds.cern.ch/record/1542341
[21] ATLAS Collaboration, 2013 *Phys. Lett. B* **726** 120, http://arxiv.org/pdf/1307.1432
[22] ATLAS Collaboration, 2012 ATLAS-PHYS-PUB-2012-004.



(a) (b)

Figure 7. Results of study of associated VH-production with subsequent $H \to b\bar{b}$ decay. (a) The $m_{b\bar{b}}$ distribution in data after subtraction of all backgrounds except for the diboson processes. The Higgs boson signal contribution is shown both with its fitted signal strength (indicated as "best fit") and as expected for the SM cross section (indicated as μ =1.0). The size of the combined statistical and systematic uncertainty on the fitted background is indicated by the hashed band. (b) Expected (dashed) and observed (solid) 95% CL cross section upper limits, normalised to the σ_{SM}, as function of m_H for all channels and data taking periods combined. The expected upper limit is given for the background-only hypothesis. The green and yellow bands represent the 1σ and 2σ ranges of the expectation in the absence of a signal.



(a) (b)

Figure 8. (a) The local probability p_0 for a background-only experiment to be more signal-like than the observation as function of m_H for the combination of all H channels. The dashed curve shows the median expected local p_0 under the hypothesis of a SM Higgs boson production at that mass. (b) Expected (blue triangles/dashed lines) and observed (black circles/solid lines) CL_s for alternative spin-parity hypotheses assuming a 0^+ signal. The green band represents the 68% CL_s expected exclusion range for a signal with assumed 0^+. For the spin-2 hypothesis, the results for the specific 2^+ model, are shown. On the right y-axis, the corresponding numbers of Gaussian standard deviations are given, using the one-sided convention.